PROCEEDINGS OF SPIE

1st Canterbury Workshop on

Optical Coherence Tomography and Adaptive Optics

Adrian Podoleanu
Editor

8–10 September 2008
Canterbury, Kent, United Kingdom

Organised by
School of Physical Sciences, University of Kent (United Kingdom)

Coorganised by
HIRESOMI—Marie Curie Early Stage Training Consortium • National University of Ireland, Galway (Ireland)
University of Porto (Portugal) • Imagine Eyes (France) • Multiwave Photonics (Portugal)

Sponsored by
European Commission, Marie Curie Actions • Imagine Eyes (France) • Michelson Diagnostic (United Kingdom) • Multiwave Photonics (Portugal) • The Ratiu Family Charitable Foundation (United Kingdom) Santec (Japan) • Superlum, Diodes, Ltd. (Russia) • Thorlabs, Inc. (United Kingdom) • University of Kent (United Kingdom)

Published by
SPIE

Volume 7139

Proceedings of SPIE, 0277-786X, v. 7139

1st Canterbury Workshop on Optical Coherence Tomography and Adaptive Optics
edited by Adrian Podoleanu, Proc. of SPIE Vol. 7139, 713901 · © 2008 SPIE
CCC code: 0277-786X/08/$18 · doi: 10.1117/12.823527

The papers included in this volume were part of the technical conference cited on the cover and title page. Papers were selected and subject to review by the editors and conference program committee. Some conference presentations may not be available for publication. The papers published in these proceedings reflect the work and thoughts of the authors and are published herein as submitted. The publisher is not responsible for the validity of the information or for any outcomes resulting from reliance thereon.

Please use the following format to cite material from this book:
Author(s), "Title of Paper," in *1st Canterbury Workshop on Optical Coherence Tomography and Adaptive Optics*, edited by Adrian Podoleanu, Proceedings of SPIE Vol. 7139 (SPIE, Bellingham, WA, 2008) Article CID Number.

ISSN 0277-786X
ISBN 9780819473806

Published by
SPIE
P.O. Box 10, Bellingham, Washington 98227-0010 USA
Telephone +1 360 676 3290 (Pacific Time) · Fax +1 360 647 1445
SPIE.org

Printed in the United States of America.

Publication of record for individual papers is online in the SPIE Digital Library.

SPIEDigitalLibrary.org

Paper Numbering: Proceedings of SPIE follow an e-First publication model, with papers published first online and then in print and on CD-ROM. Papers are published as they are submitted and meet publication criteria. A unique, consistent, permanent citation identifier (CID) number is assigned to each article at the time of the first publication. Utilization of CIDs allows articles to be fully citable as soon they are published online, and connects the same identifier to all online, print, and electronic versions of the publication. SPIE uses a six-digit CID article numbering system in which:

- The first four digits correspond to the SPIE volume number.
- The last two digits indicate publication order within the volume using a Base 36 numbering system employing both numerals and letters. These two-number sets start with 00, 01, 02, 03, 04, 05, 06, 07, 08, 09, 0A, 0B … 0Z, followed by 10-1Z, 20-2Z, etc.

The CID number appears on each page of the manuscript. The complete citation is used on the first page, and an abbreviated version on subsequent pages. Numbers in the index correspond to the last two digits of the six-digit CID number.

Contents

Conference Committees

Conference Chair and Marie Curie Coordinator

Adrian Podoleanu, University of Kent (United Kingdom)

International Organising Committee

Peter E. Andersen, Technical University of Denmark (Denmark)
Nicolas Chateau, Imagine Eyes, Paris (France)
Tatyana Cherezova, Active Optics Ltd, Moscow (Russian Federation)
Chris Dainty, National University of Ireland, Galway (Ireland)
Aristide Dogariu, University of Central Florida, Orlando, Florida (United States)
Wolfgang Drexler, Cardiff University, Cardiff (United Kingdom)
Costel Flueraru, National Research Council Canada, Ottawa (Canada)
Thomas Glynn, National University of Ireland, Galway (Ireland)
Fabrice Harms, Imagine Eyes, Paris (France)
Joseph Izatt, Duke University (United States)
Dean Johnson, Haag-Streit (United Kingdom)
Peter Koch, Thorlabs Luebeck (Germany)
Antonio Lobo, Multiwave Photonics, Porto (Portugal)
Donald Miller, Indiana University (United States)
Carla Rosa, University of Porto (Portugal)
Richard Rosen, New York Eye and Ear Infirmary (United States)
Jose Salcedo, Multiwave Photonics, Porto (Portugal)
David Sampson, University of Western Australia, Crawley (Australia)
Jose Luis Santos, University of Porto (Portugal)
Ruikang Wang, Oregon Health and Science University (United States)
Maciej Wojtkowski, Torun University (Poland)

Local Organising Committee Chair

George Dobre, University of Kent (United Kingdom)

Local Organising Committee

Pat Douglas, University of Kent (United Kingdom)
Maggie Francis, University of Kent (United Kingdom)
Michael Hughes, University of Kent (United Kingdom)
David Jackson, University of Kent (United Kingdom)
James Redmond, University of Kent (United Kingdom)
Simon Tuohy, University of Kent (United Kingdom)

Session Chairs

1 OCT Microscopy
Robert Huber, Ludwig-Maximilians-Universität München (Germany)

2 OCT in the Clinic
Jannick Rolland, University of Central Florida (United States)

3 OCT Technology
David Sampson, University of Western Australia (Australia)

4 Optical Sources I
Antonio B. Lobo Ribeiro, Multiwave Photonics S.A. (Portugal)

5 Optical Sources II
Thomas Glynn, National University of Ireland, Galway (Ireland)

6 Modulation of Optical Reflectivity
Yoshiaki Yasuno, University of Tsukuba (Japan)

7 OCT for Art
Michael Pircher, Medizinische Universität Wien (Austria)

8 General Skills
Adrian Podoleanu, University of Kent (United Kingdom)

9 Adaptive Optics I
Robert Zawadzki, University of California, Davis (United States)

10 Imaging the Eye I
Christopher Dainty, National University of Ireland, Galway (Ireland)

11 Adaptive Optics II,
Donald T. Miller, Indiana University (United States)

12 Imaging the Eye II
Wolfgang Drexler, Cardiff University (United Kingdom)

Sponsors


MARIE CURIE
ACTIONS
http://ec.europa.eu/mariecurieactions


imagine eyes


Michelson
DIAGNOSTICS


multiwave


THE RATIU FAMILY
CHARITABLE FOUNDATION


santec


SUPERLUM


THORLABS


University of
Kent

Introduction

The 1st Canterbury Workshop on Optical Coherence Tomography and Adaptive Optics has been initiated as a reporting meeting of the Marie Curie Training Site (MCTS) for early stage training (EST) researchers, MEST-2005-020353 supported by the European Commission (EC) with participants from National University of Ireland, Galway, University of Porto, Imagine Eyes, Multiwave Photonics, and coordinated by the University of Kent. The reporting meeting has the generous support of the EC to gather over 20 supervisors and EST researchers to review the achievements in research of the Marie Curie Training Site.

In opening participation to this meeting to the outside world we aimed not only for a wider scientific communication exercise, but also to add education to our EST researchers by involving them in an international exchange of ideas with other specialists in their fields: optical coherence tomography (OCT) and adaptive optics (AO). At the same time, we hope that other researchers and specialists in these fields take advantage of the educational component of this meeting.

We are grateful to the sponsors who agreed to offer their generous support to transform the Marie Curie meeting into a larger size workshop with wide international participation. These industrial sponsors are innovative companies active in the field of systems and devices for OCT and AO: Imagine Eyes (France), Michelson Diagnostics (United Kingdom), Multiwave Photonics (Portugal), Thorlabs (United Kingdom), Santec (Japan), and Superlum (Russia).

We also appreciate the continuing support given by the Ratiu Family Charitable Foundation to the University of Kent in the form of bursaries enabling Romanian students to further their education in the field of biomedical imaging and we thank the Foundation for co-sponsoring this workshop.

The site of the event is the University of Kent where research in OCT dates back to 1991, when some of the precursors of spectral domain OCT, Talbot bands, and channelled spectrum low coherence interferometry for sensing were investigated.

The field of non-invasive high resolution imaging has progressed considerably in the last three years. Among the participants to the workshop we were fortunate to have leaders in the field, who have been pushing the limits of acquisition speed. We will all be interested in finding out where those limits stand today. In the last few years, spectral domain OCT led to a significant increase in the number of Mega-voxels acquired from the tissue volume, 100 times more than in time domain OCT. Using swept sources, we expect this limit to exceed 350 Mega-voxels, while good

images of the retina at 122 Mega-voxels have been demonstrated so far[1]. The time to generate an en-face image in spectral domain OCT has also decreased, but we have not achieved as yet the capability of resonant scanning time domain OCT. A steady flow of research is manifest in improved resolution: in depth by OCT, and lateral by AO. In a B-scan generated by spectral OCT, we have recently seen the first demonstration of AO correction on shrinking the depth profile of the confocal microscope in the retina, however we are still far from achieving an ultimate resolution of 50 microns in the in vivo retina.

How will the two technologies, OCT and AO, look when this limit is finally achieved? How will they be best combined? These are stimulating challenges for our continuing research in pushing the limits of our capabilities.

We hope that the 1st Canterbury Workshop in Optical Coherence Tomography and Adaptive Optics will contribute towards advancing the frontier of knowledge in OCT and AO beyond the 'natural' limits which appear to be imposed by current technology.

Adrian Podoleanu
Conference Chair and Marie Curie Coordinator

[1] A. Gh. Podoleanu, R. B. Rosen, "Combinations of techniques in imaging the retina with high resolution," *Progress in Retinal and Eye Research*, Vol. 27, No. 4, 464-499 (2008).

Can normal lymph node architecture be characterised by optical coherence tomography?

R.A.McLaughlin[a], L.Scolaro[a], B.R.Klyen[a], S.Hamza[b], P.Robbins[c], C.Saunders[b,d], D.D.Sampson[a]
[a]Optical+Biomedical Engineering Laboratory, Uni. Western Australia, Crawley WA 6009, Australia
[b]Sir Charles Gairdner Hospital, Crawley WA 6009, Australia
[c]PathWest QEII Medical Centre, Crawley WA 6009, Australia
[d]School of Surgery, Uni. Western Australia, Crawley WA 6009, Australia

ABSTRACT

Assessment of lymph node involvement is a key prognostic marker in early breast cancer. This paper demonstrates the ability of optical coherence tomography (OCT) to characterise the micro-architecture of healthy, non-cancerous lymph nodes. OCT is shown to differentiate stroma, cortex and adipose tissue. Characteristic patterns are also identified for germinal centres and blood vessels within the node. Results are correlated against a histopathological gold standard.

Keywords: breast cancer, lymph node, optical coherence tomography, OCT.

1. INTRODUCTION

Breast cancer is the most commonly diagnosed cancer in women in the USA, with an incidence rate of 117.7 per 100,000 women [1]. In England, over 38,000 cases are diagnosed each year [2]. A critical stage in the management of cancer is to assess the spread (metastasis) of the malignancy to the lymphatic system. The lymphatic system is a network of vessels and lymph nodes throughout the body which forms a key part of the immune system.

A common surgical option to evaluate lymph node involvement is axillary clearance. This involves removal of some or all of the 25-30 lymph nodes from the axilla (armpit). The excised lymph nodes are examined using histopathological techniques to identify the presence of malignant cells. However, this results in the excision of many healthy (non-cancerous) lymph nodes and approximately 26% of patients will suffer lymphoedema [3]. Lymphoedema is caused by an accumulation of lymph (fluid) in the tissue, and manifests as a chronic swelling of the arm, breast or chest wall.

Optical coherence tomography is an optical imaging modality, using coherence-gated light in the near infrared spectrum. It has been used to obtain high-resolution images of the structural changes caused by cancer in the gastrointestinal tract [4][5], breast [6], biliary system [7] and cervix [8]. Recently, Luo et al. [9] proposed using OCT in the assessment of axillary lymph nodes. OCT provides the possibility of an imaging-based optical biopsy method for determining lymph node involvement. If performed in vivo, such a tool could potentially avoid the unnecessary excision of healthy lymph nodes; thus, reducing the incidence of complications such as lymphoedema.

When cancer metastasises to a lymph node, it disrupts the node's normal micro-architecture. In this paper, we describe the use of OCT to characterise the micro-architecture of excised normal (non-cancerous) lymph nodes. This work is an important preliminary step in establishing the feasibility of using OCT to optically identify cancerous lymph nodes.

2. EXPERIMENT

For this study, 18 lymph nodes were obtained from 13 patients undergoing either axillary clearance or sentinel lymph node biopsy. Within 10 minutes of excision, the fresh (unfixed) tissue was dissected into 2mm slices. Each slice was imaged using a time-domain OCT system with a source centre wavelength of 1320nm and full-width-half-maximum bandwidth of 101nm. Axial and lateral resolutions of the system were ~11μm. After scanning, each sample was immediately fixed in formalin and underwent histological assessment using Haematoxylin and Eosin (H&E) staining.

Image registration was then performed between the 3D OCT and 2D histology. Custom visualisation software was implemented in C++ on a Windows platform to enable the arbitrary rotation, translation and zooming of the 3D OCT data. This enabled the H&E image to be matched against the optimal 2D plane extracted from the 3D OCT data.

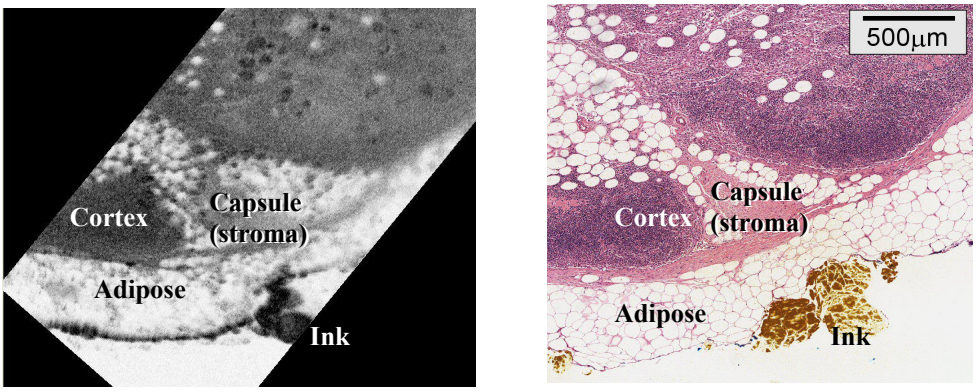

Figure 1: (Left) OCT image of lymph node. (Right) H&E histology: showing lymph cortex, adipose and stroma.

3. RESULTS AND DISCUSSION

Figure 1 demonstrates the ability of OCT to differentiate the primary tissue types found in lymph nodes: stroma, cortex and adipose (fat). The stroma consists of fibrous tissue forming the lymph node capsule, and also the delicate trabeculae which extend into the node parenchyma. The cortex is the outer portion of the lymph node. The dark staining visible in the H&E stained image is due to the high concentration of lymphocytes found in the cortex. Lymphocytes are a type of white blood cell produced in the lymph node and play a critical role in the body's immune system. The adipose tissue appears as a white area with a characteristic honeycomb structure, which is also evident in the histological images.

Figure 2 shows a cross-sectional image through two node-related blood vessels. The lymph node contains a network of lymphovascular spaces that allow the various cellular components of the immune system to enter and depart the node. Blood vessels are characterised by a dark ring surrounding an area of low back-reflection.

A non-cancerous reactive lymph node is shown in Figure 3, with prominent 'secondary' lymphoid follicles containing germinal centres within the cortex. Broadly speaking, secondary 'active' lymphoid follicles form in the cortex as part of the B-cell immune response to antigens. Under H&E staining, they are characterised by a pale germinal centre, encircled by a darker mantle zone of lymphocytes. Under OCT scanning, the circular structure of the germinal centre can be seen.

Several artefacts were observed during imaging. Adipose tissue often resulted in an increased back-reflection signal from deeper tissue. This was evidenced as dark spots (high reflection) further into the A-scan. This artefact can also be seen in the images of [9]. The mechanism for this effect has not yet been verified and will require further investigation. Additionally, the image quality was noted to deteriorate deeper in the tissue due to the cumulative effects of scattering, absorption and beam spread.

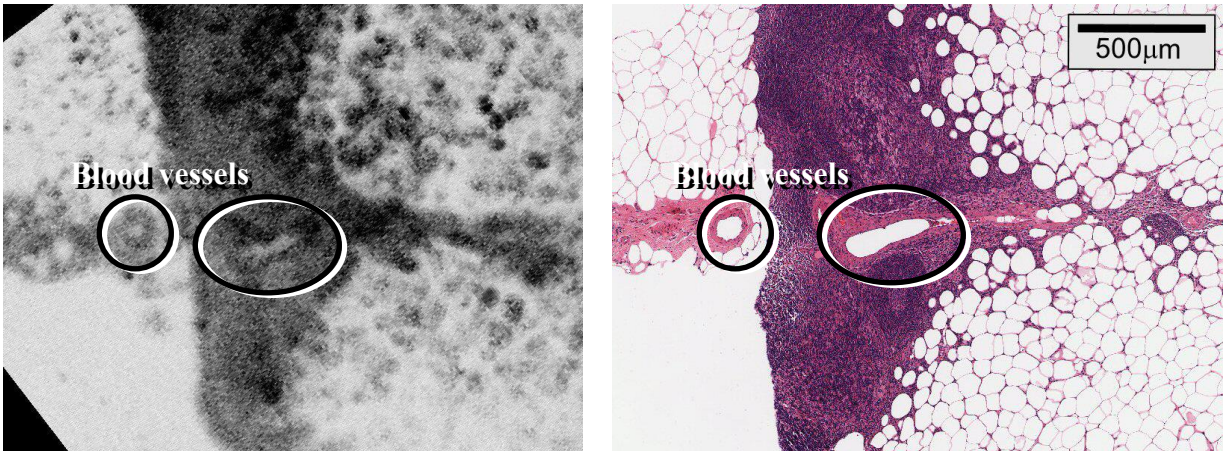

Figure 2: (left) OCT and (right) H&E histology showing blood vessels.

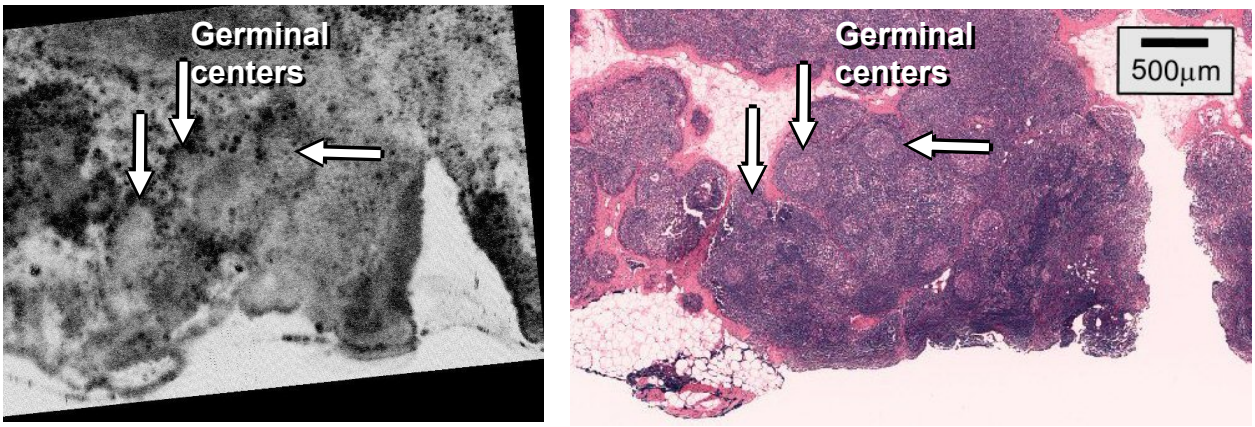

Figure 3: (left) OCT and (right) H&E histology showing lymph germinal centres and mantles.

4. CONCLUSION

In this paper, we have demonstrated the ability of OCT to image the micro-architecture of normal lymph nodes, with correlation against a histological gold standard. OCT was seen to differentiate tissue types such as cortex, stroma and adipose. In addition, characteristic patterns have been identified for microvasculature and germinal centres. Future work will focus on characterising changes in the micro-architecture due to the presence of cancer.

REFERENCES

[1] U.S. Cancer Statistics Working Group, "United States cancer statistics: 2004 incidence and mortality". Atlanta: U.S. Department of Health and Human Services, Centers for Disease Control and Prevention and National Cancer Institute (2007).

[2] National Statistics, "Cancer statistics registrations: registrations of cancer diagnosed in 2005, England", Series MB1(36), (2006).

[3] Erickson V.S., Pearson M.L., Ganz P.A., Adams J., Kahn K.L., "Arm edema in breast cancer patients", Journal of the National Cancer Institute 93(2), 96-111 (2001)

[4] Bouma B.E., Tearney G.J., Compton C.C., Nishioka N.S., "High-resolution imaging of the human esophagus and stomach in vivo using optical coherence tomography", Gastrointestinal Endoscopy 51(4), 467-474 (2000).

[5] Evans J.A. et al., "Optical coherence tomography to identify intramucosal carcinoma and high-grade dysplasia in Barrett's Esophagus", Clinical Gastroenterology and Hepatology 4, 38-43 (2006).

[6] Boppart S.A., Luo W., Marks D.L., Singletary K.W., "Optical coherence tomography: feasibility for basic research and image-guided surgery of breast cancer", Breast Cancer Research and Treatment 84, 85–97 (2004)

[7] Poneros J.M., Tearney G.J., Shiskov M., Kelsey P.B., Lauwers G.Y., Nishioka N.S., Bouma B.E., "Optical coherence tomography of the biliary tree during ERCP", Gastrointestinal Endoscopy 55(1), 84-88 (2002)

[8] Escobar P.F., Belinson J.L., White A., Shakhova N.M., Feldchtein F.I., Kareta M.V., Gladkova N.D., "Diagnostic efficacy of optical coherence tomography in the management of preinvasive and invasive cancer of uterine cervix and vulva", International Journal of Gynecological Cancer 14, 470-474 (2004)

[9] Luo W., Nguyen F.T., Zysk A.M., Ralston T.S., Brockenbrough J., Marks D.L., Oldenburg A.L., Boppart S.A., "Optical biopsy of lymph node morphology using optical coherence tomography", Technology in Cancer Research & Treatment 4(5), 539-547 (2005).

A first demonstration of audio-frequency optical coherence elastography of tissue

Steven G. Adie, Sergey A. Alexandrov, Julian J. Armstrong, Brendan F. Kennedy and David D. Sampson
Optical+Biomedical Engineering Laboratory, School of Electrical, Electronic & Computer Engineering, The University of Western Australia, 35 Stirling Highway, Crawley, Western Australia 6009, Australia

ABSTRACT

Optical elastography is aimed at using the visco-elastic properties of soft tissue as a contrast mechanism, and could be particularly suitable for high-resolution differentiation of tumour from surrounding normal tissue. We present a new approach to measure the effect of an applied stimulus in the kilohertz frequency range that is based on optical coherence tomography. We describe the approach and present the first *in vivo* optical coherence elastography measurements in human skin at audio excitation frequencies.

Keywords: Elastography, optical coherence tomography, tissue mechanical properties

1. Introduction

Optical coherence elastography (OCE) reported to date has been based on speckle-tracking techniques, and has employed predominantly quasi-static mechanical loading of tissue to quantitatively assess local tissue motion [1-4]. In this paper, we present a new approach to OCE suitable for the quantitative measurement of tissue mechanical properties in the hundred Hertz to kilohertz frequency range.

2. Theory and experimental method

Consider an interferometric signal generated by a reference light beam combining with light backscattered from particles undergoing harmonic displacement along the optical (z) axis. At frequencies up to several kHz (with corresponding sound wavelength $\Lambda \sim 1$m), particles in a medium (of typical thickness ~ 1mm) can be expected to move in phase with each other. The dynamic interferometric signal amplitude of interest depends not only on the scatterer's vibration amplitude but also on the quasi-static phase of the interferometer, which in turn is governed by the precise differential axial position of the particle relative to the reference path in the interferometer. This unwanted dependence of the dynamic displacement on the quasi-static displacement is generally known as interferometric signal fading [5,6]. It can be overcome by various means, e.g., by polarization-based optical quadrature detection [7].

A schematic of the experimental fibre-based, time-domain OCT system utilizing balanced optical quadrature detection is presented in Fig. 1. A broadband source with a near-Gaussian spectrum centred at 1334nm with 3dB bandwidth of 42nm was employed, and the sample arm utilized a triplet lens (f = 30mm) to focus the beam through a glass window that provided a rigid platform upon which the samples were placed. Dynamic compression was applied to the sample, as indicated in Fig. 1 (inset), with a PZT actuator. The frequency-domain optical delay line (FD-ODL) was operated off-pivot to acquire conventional OCT images using a carrier frequency of 1150 Hz [8] and on-pivot when the vibration of sample scatterers generated the carrier frequency.

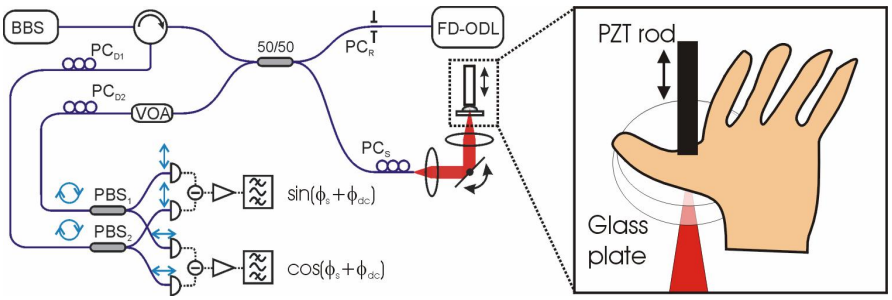

Figure 1: Schematic of the fibre-based OCT system employing balanced optical quadrature detection and the experimental geometry.

The detected photocurrents in the orthogonal polarization channels (see Fig. 1), denoted by the subscripts 1 and 2 can be expanded as a series of Bessel functions [6], resulting in the following equation:

$$i_1(z,t) = 2\rho\sqrt{I_R I_S}\left\{\cos\phi_{DC}\left[J_0(\phi_s) + 2\sum_{n=1}^{\infty} J_{2n}(\phi_s)\cos(2n\Omega t)\right] + \sin\phi_{DC}\left[2\sum_{n=0}^{\infty} J_{2n+1}(\phi_s)\sin\left((2n+1)\Omega t\right)\right]\right\}, \quad (1)$$

$$i_2(z,t) = 2\rho\sqrt{I_R I_S}\left\{\sin\phi_{DC}\left[J_0(\phi_s) + 2\sum_{n=1}^{\infty} J_{2n}(\phi_s)\cos(2n\Omega t)\right] + \cos\phi_{DC}\left[2\sum_{n=0}^{\infty} J_{2n+1}(\phi_s)\sin\left((2n+1)\Omega t\right)\right]\right\}, \quad (2)$$

where ρ is the detector responsivity, I_S and I_R are the sample and reference optical intensities, respectively, ϕ_{DC} is the quasi-static interferometric phase (modulo 2π) governed by the axial position of the particle, $\phi_s = \frac{4\pi}{\lambda} d(z,\Omega)$, where λ is the mean optical wavelength in the medium, d is the local, generally frequency-dependent, amplitude of vibration, Ω is the angular vibration frequency and J_n is the n^{th} order Bessel function of the 1st kind corresponding to the n^{th} order harmonic of the excitation frequency. It is readily seen from Eqs. (1) and (2) that the value of ϕ_{DC} alters the detected signal and has the potential to produce distortions in the dynamic signal. In channel 1 (Eq. (1)), the even harmonics of the signal fade when $\phi_{DC} = \pi/2$; conversely, in channel 2, the odd harmonics of the signal fade when $\phi_{DC} = \pi/2$.

The objective of the OCE scheme presented here is to deduce the absolute vibration amplitude (i.e., dynamic displacement) of the scatterer through an interferometric measurement of ϕ_S. In our approach, the theoretical values of J_3/J_1 are used to map the experimentally measured J_3/J_1 ratios to vibration amplitude, as described previously [6]. Furthermore, we use the ratio of J_4/J_2 to extend the unambiguous range of operation to beyond approximately λ/3; the first calibration range given by $J_4/J_2 < -4.696$dB and the second by $J_4/J_2 \geq -4.696$dB. At an operating mean wavelength of λ =1300 nm, this permits measurement of absolute vibration amplitudes of up to about 0.6μm (optical depth).

Analysis of the full-fringed digitized data was carried out in post-processing, separately for each channel. We calculated intensity images for four separate harmonic frequencies by applying bandpass filters centred at Ω, 2Ω, 3Ω and 4Ω (producing in total eight frames from the two detection channels). These frames were then separately demodulated utilizing the Hilbert transform and the resulting orthogonal envelopes at each vibration harmonic were incoherently combined. The resulting four frames, immune to signal fading, were used to produce a frame containing local vibration amplitude using the ratio J_3/J_1 as described above.

3. Results and discussion

Figure 2 presents results of *in vivo* measurements of human thick skin (on the palm) obtained by compressing the "webbing" between the thumb and index finger between the PZT rod and the sample-arm window. The OCT image (without applied vibration) consists of 32 A-scans taken over a lateral scan range of 0.8 mm. The lateral spacing was relatively large compared to the lateral resolution in order to obtain an adequate field of view with the relatively slow A-scan rate. The vibration amplitude measurement consisted of 8 A-scans centred at the same lateral position, but over a 0.4-mm range, again to avoid boundary effects. A relatively uniform signal from the skin surface to z = 0.2 mm optical depth can be distinguished in both the OCT image (Figure 2a) and the average A-scan (Figure 2b), which corresponds to a layer with low vibration amplitude in Figure 2c. This layer is attributed to the stratum corneum, which displays negligible vibration amplitude due to its tight coupling to the rigid glass window and its low compressibility.

Below the stratum corneum, the OCT image does not show any clear boundary between skin layers until a depth of approximately 0.85 mm. In contrast, the vibration amplitude traces show a distinct difference in slope at about 0.65 mm that is replicated over the range of PZT drive voltages. The change in slope of the vibration amplitude traces indicates two layers of different compressibility, with the deeper layer, with greater slope, being relatively more compressible. We attribute these layers to the epidermis and dermis respectively, which are known to have distinct mechanical properties. Beyond a depth of z = 0.85 mm, the signal is most likely due to the multiple scattering background. The discontinuity in

the vibration traces of Figure 2d is a stitching artefact occurring at the intersection of the calibration curves (when the vibration amplitude is approximately λ/3). The dynamic OCE method put forward here naturally detects the axial motion of scatterers. Accordingly, our experimental geometry was designed so that, in each case, the PZT transducer applied even pressure to the sample coaxially with the optical beam. Further work is required to establish the feasibility of accurately detecting vibration amplitude in the presence of lateral scatterer motion, such as when shear waves are excited.

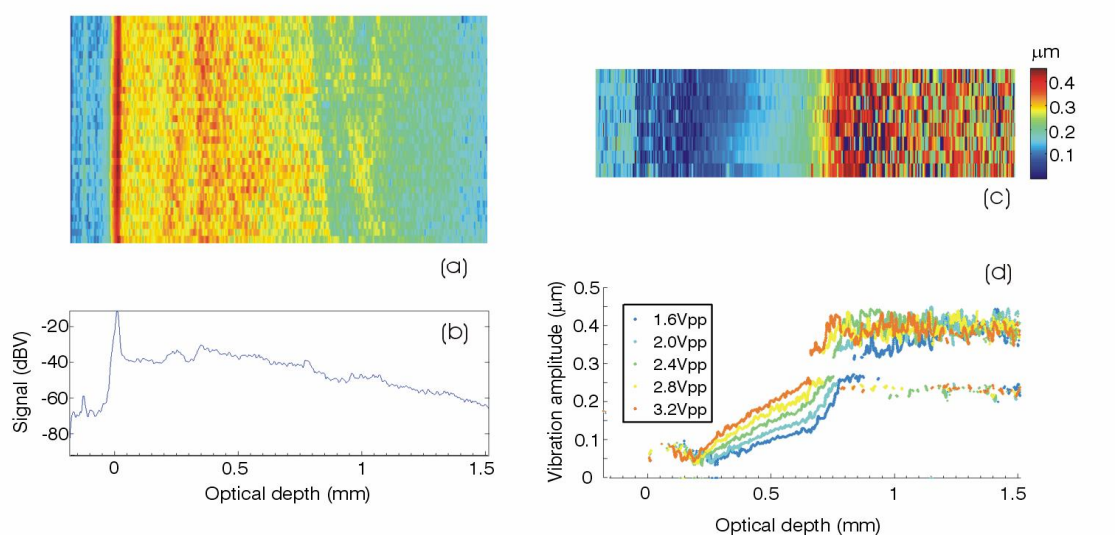

Figure 2: OCT A-scan and OCE-derived vibration amplitude versus optical depth for human skin *in vivo*: (a) OCT image without applied vibration; (b) Average A-scan; (c) Vibration amplitude image for PZT drive voltage of 2.4Vpp; and (d) Average vibration amplitude for various PZT drive voltages.

4. Conclusions

In conclusion, we have presented a new dynamic OCE method suited to quantitative displacement assessment at frequencies in the hundreds of Hertz to kilohertz regime. The method was able to distinguish the layers in a 3-layer phantom with different elasticity based on differences in the measured vibration amplitude in each layer. The first quantitative *in vivo* OCE measurements of human skin clearly distinguish layers based upon their mechanical response. In these measurements, increased driving amplitude produced a higher gradient of vibration amplitude vs. depth, indicating greater compression of compliant layers. The technique can be adapted to perform high-spatial resolution vibration-based spectroscopy, where the excitation frequency is tuned over the 100 Hz to 10 kHz range. Such spectroscopic measurements based on the frequency-dependent mechanical response of tissue could potentially enhance the capability of OCE in diagnosis of a range of medical conditions, including tumours and arterial plaques.

References

[1] J. M. Schmitt. OCT elastography: imaging microscopic deformation and strain of tissue. Optics Express, 3(6):199–211, 1998.

[2] R. C. Chan, A. H. Chau, W. C. Karl, S. Nadkarni, A. S. Khalil, N. Iftimia, M. Shishkov, G. J. Tearney, M. R. Kaazempur-Mofrad, and B. E. Bouma. OCT-based arterial elastography: robust estimation exploiting tissue biomechanics. Optics Express, 12(19):4558–4572, 2004.

[3] J. Rogowska, N. A. Patel, J. G. Fujimoto, and M. E. Brezinski. Optical coherence tomographic elastography technique for measuring deformation and strain of atherosclerotic tissues. Heart, 90(5):556–562, 2004.

[4] H. J. Ko, W. Tan, R. Stack, and S. A. Boppart. Optical coherence elastography of engineered and developing tissue. Tissue Engineering, 12(1):63–73, 2006.

[5] E. Udd. Fiber optic sensors : an introduction for engineers and scientists. Wiley, New York, 1991.

[6] O. Sasaki and H. Okazaki. Sinusoidal phase modulating interferometry for surface profile measurement. Applied Optics, 25(18):3137–3140, 1986.

[7] Y. Zhao, Z. Chen, Z. Ding, H. Ren, and J. S. Nelson. Real-time phase-resolved functional optical coherence tomography by use of optical Hilbert transformation. Optics Letters 27(2): 98-100, 2002.
[8] A. V. Zvyagin, E. D. J. Smith, D. D. Sampson. Delay and dispersion characteristics of a frequency-domain optical delay line for scanning interferometry. Journal of the Optical Society of America A. 20(2):333-341, 2003.